

Manganese Concentration Mapping with Magnetic Resonance and Positron Emission Tomography

Geoffrey Topping¹, Andrew Yung², Paul Schaffer³, Piotr Kozlowski², Thomas Ruth³, and Vesna Sossi¹

¹Physics and Astronomy, University of British Columbia, Vancouver, British Columbia, Canada, ²MRI Research Centre, University of British Columbia, Vancouver, British Columbia, Canada, ³Nuclear Medicine, TRIUMF, Vancouver, British Columbia, Canada

Introduction

Manganese-enhanced MRI is useful for measuring neuronal activity, due to accumulation of Mn in cells via voltage gated calcium channels (Lin, 1997, MRM). However, quantification and validation of results *in vivo* are challenges for MRI. As well, MEMRI generally requires pharmacological doses of Mn, which may alter the biological systems being studied. The radionuclide Mn-52 is suitable as a positron emission tomography radiotracer, and can be used for MEMRI result validation due to the reliable quantification of PET, with or without pharmacological doses of Mn. In this work, Mn-52 has been produced and imaged in the rat brain. MRI Mn concentration maps in the rat brain have been acquired, and are compared with PET Mn-52 concentration images.

Methods

Natural Cr foil (Goodfellow) was irradiated with 12.5 MeV protons to produce Mn-52. Mn was separated from Cr by column chromatography with AG 1x8 anion exchange resin (BioRad), then redissolved in 10 mM phosphate-buffered saline. 12 MBq of Mn-52 in 2 ml volume was injected over 10 minutes into a Sprague-Dawley rat tail vein under isoflurane anesthesia (on the order of ng/kg chemically). From 30 to 60 min, and 75 to 90 min post injection, images were acquired with a Focus 120 small animal microPET system (Siemens/Concorde). Coincidence energy window was 450-600 keV and timing window was 5 ns. The image was reconstructed by filtered back projection as a single frame with $0.433 \times 0.433 \text{ mm}^2$ pixels, 0.796 mm slice thickness, 128x128x95 voxels, 76 mm axial FOV, and $55 \times 55 \text{ mm}^2$ in-plane FOV. Scatter and attenuation corrections were applied, with attenuation maps calculated by segmenting a 10 min Co-57 rotating point source transmission image.

40 mg/kg MnCl₂ in phosphate-buffered saline was intraperitoneally injected in a Sprague-Dawley rat under isoflurane anesthesia. Pre-, 70 post-, and 120 min post-injection, T1 maps were acquired with a 7 T small animal MR system (Bruker) using a sagittal multi-slice FLASH-based Look-Locker sequence (Chuang, 2006, MRM) (with volume-coil transmit and surface coil-receive, inversion TR=10 s, TE=3 ms, inter-excitation TR=150 ms, 40 images per inversion, $\alpha=20$ deg, inversion delay = 10.43 ms, matrix size 128x72, FOV=4x2.25 cm², slice thickness 625 μm , 17 slices, and acquisition time 12 min). Rectal temperature was maintained at 36.9 +/- 0.2 C during T1 mapping. Mn relaxivity calibration data were also acquired by measuring T1 by non-imaging inversion recovery for varying concentrations of MnCl₂ in saline. Using these data, *in-vivo* Mn concentration maps were generated.

Results

Rat Mn-52 PET images are shown in Fig. 1. A region of interest (9x4x1 voxels) was placed on the pituitary activity peaks in the transverse image plane, which had average voxel Mn-52 concentrations of 32 kBq/cc at 30-60 min, and 34 kBq/cc at 75-90 min.

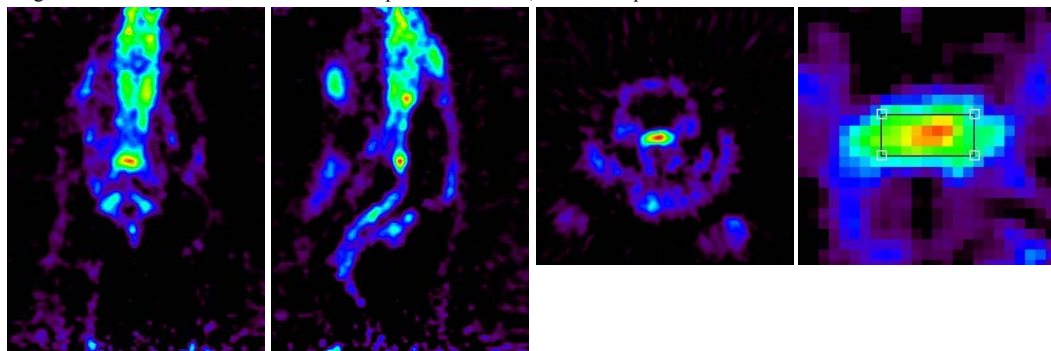


Fig. 1 - Mn-52 PET image of rat head. Coronal (left), sagittal (centre-left), and transaxial (centre-right) slices through the pituitary are scaled 0 (black) to 35 kBq/cc (red). Zoomed transaxial (right) slice with region of interest is scaled 0 (black) to 45 kBq/cc (red).

Mn relaxivity at 36.9 C was estimated to be $4.30 \text{ s}^{-1} \text{ mM}^{-1}$ at 36.9 C in saline. A rat Mn MRI-derived concentration map is shown in Fig. 2, with the T1 maps from which it was derived. Regions of interest (10x4x1 voxels) was placed on the pituitary concentration peak in the composite transverse images, and had an average Mn concentration of 1.6 μM at 70 min and 2.1 μM at 120 min, corresponding to R1 changes of 0.00036 s^{-1} at 70 min and 0.00050 s^{-1} at 120 min.

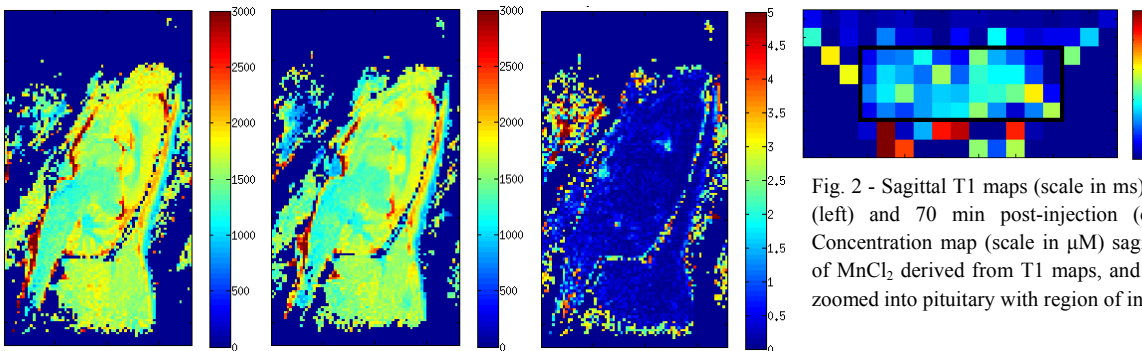


Fig. 2 - Sagittal T1 maps (scale in ms) of rat brain at baseline (left) and 70 min post-injection (centre-left) of MnCl₂. Concentration map (scale in μM) sagittal view (centre-right) of MnCl₂ derived from T1 maps, and transverse view (right) zoomed into pituitary with region of interest.

Both MRI and PET-derived concentration maps show little short-term uptake in the majority of the brain volume. The pituitary appears prominently in both modalities, with better spatial resolution in MR. Another localized peak is seen anterior and superior to the pituitary in the MR-derived map, and appears faintly in the PET image. Accumulations of Mn outside the brain are unclear with MR, due to noise outside the sensitive range of the surface coil and lack of MR signal from bone. PET clearly shows a large distribution of Mn-52 accumulation anterior to the brain, in the bones surrounding the brain and spinal cord, in the throat, and the lower jaw. Similar results between modalities within the brain suggest that PET and MR are measuring results of the same biological processes, and that pharmacological doses of Mn do not drastically change the short-term Mn accumulation pattern after systemic administration.